SM Journal of Biomedical Engineering ISSN: 2573-3702

Research Article

Dosimetric Impact of Vascular Access Ports in Proton Therapy

Michael S. Gossman[1,2], Tianyu Zhao[3], and Yao Hao[3]

[1]Regulation Directive Medical Physics, New Albany, IN 47150, USA

[2]Washington University School of Medicine, Proton Therapy Center, St. Louis, MO 63108, USA

Abstract

Implanted ports are commonly used to deliver chemotherapy as part of chemoradiotherapy. The Department of Radiation Oncology must consider the impact of materials of construction of implanted ports on the alteration of radiation beam(s). The purpose of the current investigation was to evaluate the dosimetric consequences of having commercially available ports in the path of various therapeutic proton radiation beams. Proton beam range and intensity profiles were analyzed for changes when a vascular access port was introduced into the path of the beam. Clinically available energies were considered from a cyclotron at 51 MeV, 100 MeV, 150 MeV and 200 MeV. Three (n=3) different commercially available ports were investigated, including models from two different manufacturers. Each port was composed primarily of, or entirely of, plastic. Having ports in the therapeutic beam caused the Bragg peak to shift to a shallower depth, moving the proton beam range -0.6 cm to -1.4 cm. A high drop in profile intensity was observed at all proton beam energies, dropping the intensity from a normally flat profile down -67% to -96%. The full-width half maximums (FWHMs) of the dose drop region varies between -1.70 cm and -2.60 cm. Each port resulted in observed variations, with shifts more pronounced at lower proton beam energies. No single port yielded results that suggest the ability to achieve optimal proton beam radiation therapy dosing when the beam traverses the port. Clinical strategies for avoidance may include placement of dense implants at alternate site away from the treatment area, removal of dense implants, or adjustment of the gantry angle to avoid the implant altogether. The current study may be considered by physicians and medical physicists who are responsible for chemoradiotherapy, PBT planning, dosing, and administration to optimize care delivery in this setting.

Keywords: Attenuation; Bragg peak; Dose; Proton

Introduction

There are many departments in the hospital that benefit from the use of vascular access ports. Ports are typically implanted subcutaneously in the upper chest region, with the catheter positioned at or near the cavo-atrial junction. Since 1969, ports have been chosen as a means for routine sampling of blood and for delivery of intravenous medications, anesthetics, and chemotherapeutic agents [1-5]. It is for this reason that patients with cancer routinely have vascular access ports implanted. Concurrent use of radiotherapy along with chemotherapy (radiochemotherapy) is the established standard of care for many locally advanced solid tumors including gastrointestinal malignancies, head and neck cancers, gynecological cancers, and lung cancers, among others [6]. Considering the common use of implanted ports to delivery chemotherapy as part of chemoradiotherapy, the Department of Radiation Oncology must consider the impact of materials of construction of implanted ports, namely, high density plastic and metal, regarding alteration of the radiation beam(s). Considerations of this alteration are ubiquitous in planning external beam radiation therapy, regardless of the specific radiation therapy modality.

Radiation therapy is commonly conducted using a medical accelerator. Accelerators have the capability of emitting x-rays or electrons. Both radiation types are emitted in high intensity beams, both of which can be shaped and focused at different beam angles to achieve the desired radiation dose distribution around the cancer target. The dose deposition from x-ray and electron radiation is very nearly an exponential decay, following the quick depth-dose peak that is characteristic of these beam types. When an object, having density greater than water, is found to be in the direct path of the intended x-ray or electron radiation, absorption of the radiation and scattering cause disturbance of the concentrating beam. This disruption exists in the form of beam intensity attenuation, alteration of the shape of the focused beam, and even the quality of the beam energy.

Research on vascular access ports involving medical accelerators revealed significant differences when comparing the dose affect from x-rays and electrons. It was determined that due to the characteristic design of ports with various composite materials having different densities, not all the port models tested demonstrated the same high gradient in dose intensity change. Nevertheless, the authors concluded that for all models tested, the changes may be clinically significant and should be considered in x-ray beam radiation therapy planning [7-15].

Submitted: 01 July 2023 | **Accepted:** 24 July, 2023 | **Published:** 26 July, 2020

***Corresponding author:** Michael S. Gossman, M.S., DABR, FAAPM, FACR, Regulation Directive Medical Physics, New Albany, IN 47150, USA

Citation: Gossman MS, Zhao T, Hao Y (2023) Dosimetric Impact of Vascular Access Ports in Proton Therapy. SM J Biomed Eng 6: 7.

Radiation therapy can also be conducted using cyclotrons to emit proton radiation beams. The dose deposition from proton radiation is quite unique by comparison to x-ray and electron radiation. Using this modality, the beam has a mostly constant intensity as it passes through the patient until the protons come to an abrupt stop. It is here that the depth-dose maximum occurs, existing as a sharp peak of increased dose, and a rapid fall-off to zero dose. For proton beams, this is referred to as the Bragg[1] peak [16]. The proton beam energy is generally defined by the range of protons. It is the precise position of the Bragg peak along with the proximal and distal peak gradients that relate the quality of the beam. Specifically, the range of the proton beam is defined at the posterior gradient Bragg peak fall-off where the dose falls to 90% of the Bragg peak dose.

The clinical use of the proton beam involves introducing variable thickness attenuators like spinning wedges or compensators into the beam, where the Bragg peak stretches out to form a longer plateau called the spread-out Bragg peak (SOBP). By expanding the sharp Bragg peak into a raised flat high dose area, clinicians can take advantage of planning for the target cancer to reside in this distance-limited range. Protons are also emitted in high intensity beams, and can be shaped and focused at different beam angles to achieve the desired radiation dose distribution around the cancer target.

Only a few studies have been found to examine dosimetric consequences of having a port in the direct path of a proton beam. It is expected that variations in the denseness of the medium would impact proton beam dose intensity and distribution [17-18]. The loss of dose intensity observed across any dense devices supports guidance from the American College of Radiology to avoid transmission through such materials where possible.[15] Zhao, L. et al. examined a single port from a breast tissue expander, finding that the metallic port can cause the Bragg peak to shift upstream [19]. In a non-clinical investigation, Basit arrived at a similar conclusion when considering vascular access port materials of construction.[20] In a mock exercise, when entering representative raw material partial composition information into a computerized treatment planning system to model, the shift in Bragg peak had a negative correlation with increasing density of the materials [20]. However, it is noted that an authentic computerized tomography (CT) scan from a port was not utilized in this study. An additional limitation of this study was the use of representative port materials, rather than commercially available ports. Therefore, it was suggested by the author that future studies are needed wherein currently available ports are tested [20].

1 The Bragg peak is a prominent peak on the plot for the energy loss of ionizing radiation during its travel through matter. For protons, the peak occurs immediately before the beam of particles come to rest. It is named after William Henry Bragg, who discovered it in 1903.[14]

The purpose of the current investigation was to evaluate the dosimetric consequences of having commercially available ports in the path of various therapeutic proton radiation beams. Computerized modeling was used from CT scans of each three actual port models, with stopping powers entered to represent the beam being used. Radiation measurements were also used for additional evaluation. Here, we present the complete analysis of the study, detailing conclusive proton beam Bragg peak shifts and the inherent range shift and intensity profile drops when ports are included in the path of the beam.

Materials and Methods

There were three (n=3) ports chosen for the study. They include the AngioDynamics® SmartPort+™ Plastic port (AngioDynamics®, Latham, NY), and two ports from Becton, Dickinson and Company® (aka: BD®, Franklin Lakes, NJ), the PowerPort® VUE M.R.I® port and PowerPort® ClearVUE® Slim port. Each are shown in Figure 1.

For radiation range measurements, an IBA Dosimetry® Gmbh (Schwarzenbruck, GERMANY) Model Zebra™ multilayer ionization chamber array with software was chosen for use. The detector system contains 180 parallel-plane ion chambers spaced 2 mm along the beam axis. The Zebra™ array was first positioned on the treatment couch and aligned with the gantry of Mevion® S250i™ proton cyclotron with Hyperscan™ (Mevion Medical Systems®, Littleton, MA).

Figure 1 (Top) AngioDynamics® SmartPort+™ Plastic port [© images courtesy of AngioDynamics®],

(Bottom) BD® PowerPort® VUE M.R.I.® port and PowerPort® ClearVUE® Slim [© images Courtesy of Becton, Dickenson and Company®]

To begin, and only for proton energies 100 MeV, 150 MeV and 200 MeV, a port was positioned on top a Solid Water™ phantom (Sun Nuclear Inc., Middleton, WI) Model 457-210 having dimensions 20 x 20 x 1.0 cm^3. After centering, the port was then overlaid by an Elasto-Gel™ sheet bolus (Southwest Technologies Inc., North Kansas City, MO) Model GS202038 with dimensions 20" x 20" x 1.0 cm. Each sandwiched set was then placed in front of Zebra™ array. For proton energies 100 MeV, 150 MeV and 200 MeV, a single spot plan was delivered. It is noted that due to the short range of the protons in the 51 MeV beam, no bolus or plastic build-up was added. It can be said initially that without the bolus present at 51 MeV, results were not ideally suited to represent expected clinical results, since there was no approximated skin present. However, measurements were taken anyway with no bolus build-up in order to reveal the similar trend in results when a port was included in the beam, regardless of whether it was under the skin or not.

Consecutive measurements were conducted for each of the three ports at each energy setting, with the port included and not included, and with the bolus on or off depending on energy. In each setup, a simple orthogonal pair of x-rays were delivered (Anterior-posterior & Lateral) from the side images of the Mevion® cyclotron, in order to ensure the port was centered in the beam. Small adjustments in the position of the couch based on these images enabled centering adjustments.

For computer modeling, the study began with a need to perform a CT scan of each port being investigated. As such, a phantom was created out of water and solid plastics to represent a patient. A CIRS Inc.® (Norfolk, VA) Model Plastic Water™ [5 cm slab PW-3030-05 (Qty=5), 2 cm slab PW-3030-02, and 1 cm slab PW-3030-01] having dimensions 30 x 30 cm^2 was stacked to 28 cm to simulate the thickness of a large patient. The phantom was loaded on the couch of a Siemens Medical Solutions® (Munich, GERMANY) Model SOMOTOM™ Edge™ CT scanner. A single port was chosen for use in the experiment and centered on top of the phantom. The port was filled with 15 mL saline using a syringe. Finally, the 1 cm bolus was again placed directly over the port to build-up the simulated patient skin thickness.

A CT scan was conducted with and without the port present. Scans were acquired using a technique of 120 kVp, with a 40 cm field-of-view (FOV) and imaged at 1.5 mm slice increments. Images were networked to a computer for treatment delivery modeling and simulation. Identical CT scans were conducted for each of the three ports investigated in this study, with the port included and not included, and with the bolus on. Proton beam irradiation modeling was conducted using RaySearch Laboratories® Model RayStation™ (Stockholm, SWEDEN) treatment planning software Version 11A. Using software tools, the port was contoured in three dimensions.

First, a single anterior-posterior beam having field size dimensions 20 x 20 cm^2 was directed through the center of the port. This setup represents a classical open field beam. Static aperture-based beams, like that of the open field, are more traditional types of setups. We introduce this beam for consideration as well as the more modern beam setup.

More recently, cyclotron machines have been invented to incorporate directing a scanning focused pencil beam. The Mevion® S250i™ proton cyclotron with Hyperscan™ is one such machine. It includes in the head of the gantry a set of dual directing internal coil magnets that can be adjusted in strength, by varying the current flow through it, to redirect the spot of focused radiation. By continual change of the magnet, the beam that exits the nozzle can be used to effectively scan over the surface, depositing dose over an area. We made use of this ability to create a second beam, which scans with a spot spacing of 2.5 mm to ultimately superimpose intensity to generate an irradiated area of 20 x 20 cm^2.

Both setups were delivered consecutively to yield changes that can be related to older cyclotrons and ones that are more modern, as offered by the Mevion® S250i™ proton cyclotron with Hyperscan™. The beam-on timer was set to 500 monitor units (MU). RayStation software was used to show the line-dose profile at proton beam energies 51 MeV, 100 MeV, 150 MeV and 200 MeV. A plot was created for each port being evaluated, for dose when no port was included as well as the line-dose profile when a specific port was included in the beam path. The depth of the line dose profiles was selected as the maximum dose depth without port.

Results

The integral depth-dose profile for each single spot proton beam was plotted, agreeing with the expectations from commissioning, and in-line with findings for similar beams on similar machines with a well-defined Bragg peak.[16-18] Each plot was examined for the deposition of dose through the entire range (90% Bragg peak dose) of the protons at depth in the water phantom, both with and without a port present in the direct path of the beam. All plots were found to resemble Figure 2.

The greatest observable difference between plots for the various energies used is that the Bragg peak exists more upstream (towards the surface) as the proton beam energy is decreased. The range change is defined by the shift in the position of the 90% posterior gradient fall-off from the Bragg peak when comparing results with the port and without the port. For example, in Figure 2 at 200 MeV for the AngioDynamics® SmartPort+™ Plastic port, the single spot range change was found to be (22.50 cm – 23.70 cm) = -1.20 cm. The single spot and open field 20 x 20 cm^2 range change results for all ports studied here are presented in Table 1

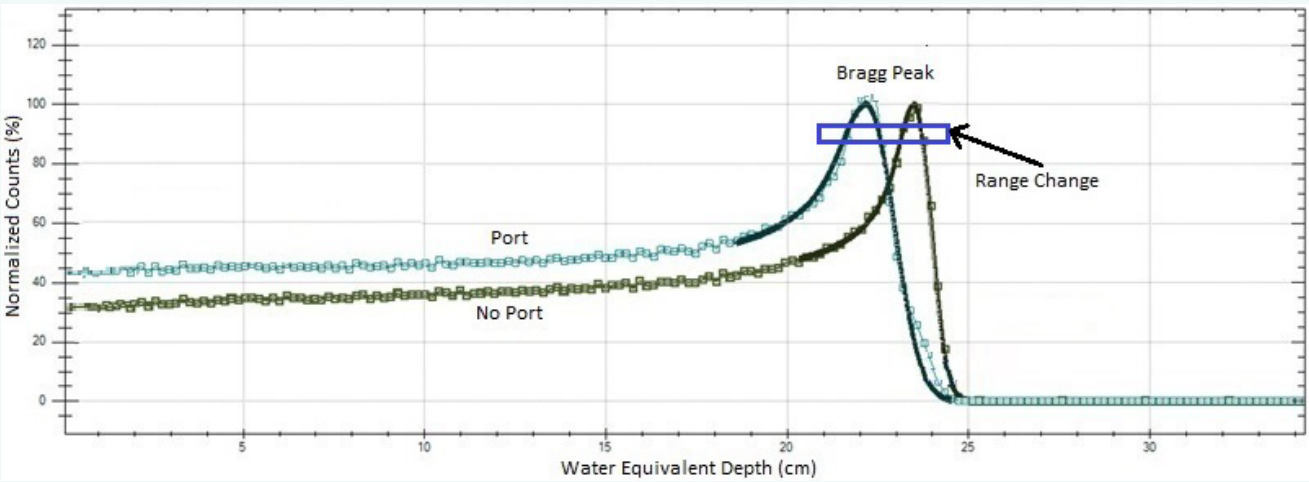

Figure 2 200 MeV proton beam range shift for an AngioDynamics® SmartPort+™ Plastic port. Solid lines are fitting curves by which range was calculated.

Table 1. Bragg peak range change for all ports at all energies.

	Single Spot Range Change				Open field Range Change			
Port	51 MeV	100 MeV	150 MeV	200 MeV	51 MeV	100 MeV	150 MeV	200 MeV
AngioDynamics® SmartPort+™ Plastic	-1.20 cm	-0.77 cm	-0.99 cm	-1.20 cm	-1.19 cm	-1.16 cm	-1.21 cm	-1.20 cm
BD® PowerPort® VUE M.R.I®	-1.38 cm	-0.96 cm	-1.15 cm	-1.23 cm	-1.32 cm	-1.27 cm	-1.32 cm	-1.26 cm
BD® PowerPort® ClearVUE® Slim	-1.05 cm	-0.60 cm	-0.88 cm	-1.10 cm	-1.04 cm	-1.03 cm	-1.05 cm	-1.10 cm

for each beam energy considered.

Finally, a high drop in profile intensity was observed at all proton beam energies. Normally, the 20 x 20 cm^2 square proton beam is flat and symmetric about the central axis of the beam. This is the case when no port is included in the beam path. However, when a port is introduced, the profile intensity drops considerably. The dose intensity profile change is defined by the change in the position of the beam profile position with the introduction of a port. A comparison of the normal profile shape and the drop in intensity when the port is included in the beam is shown in Figure 3.

As illustrated in Figure 3, the shape of the clinical profile is important when it comes to beam shaping. When modeling a beam to treat a target cancer it is important to have a uniform dose distribution around it. Such uniform distributions are made possible by making use of the rotational ability of the machine's gantry, either for static delivery of beams or via rotational arc delivery. Large dips in the beam profile due to obstruction by dense materials make uniform dose distribution challenging when creating a plan for a patient. Drastic changes in the beam intensity make it near to impossible to create an ideal computerized treatment plan that results in a beam enveloping the entire target conformally, while allowing organs-at-risk in the vicinity of the target to have dose sparing. Merely as an example, arbitrarily choosing the data at 200 MeV for the AngioDynamics® SmartPort+™ Plastic port, the profile dose change was found to be 100 % x [(65 cGy – 260 cGy)/260 cGy] = -75 %. The dose intensity profile change results for all ports studied here are presented in Table 3 for each beam energy considered. The full width half maximum (FWHM) of each dipped dose region behind each port are presented in Table 2 for all energies. With energy increasing, FWHMs increase. However, decreasing changes were observed for the dose intensity profile along the central axis.

Discussion

This study investigated the dosimetric consequences of placing a vascular access port directly in the beam of a therapeutic proton field. The ports studied were the AngioDynamics® SmartPort+™ Plastic port, BD® PowerPort® VUE M.R.I® port and PowerPort® ClearVUE® Slim port. Each were evaluated with the same equipment, methods, and metrics. For each technique, various energies of proton beams were considered, as they are clinically relevant to patients receiving cancer treatment. The proton beam energies were 51 MeV, 100 MeV, 150 MeV and 200 MeV.

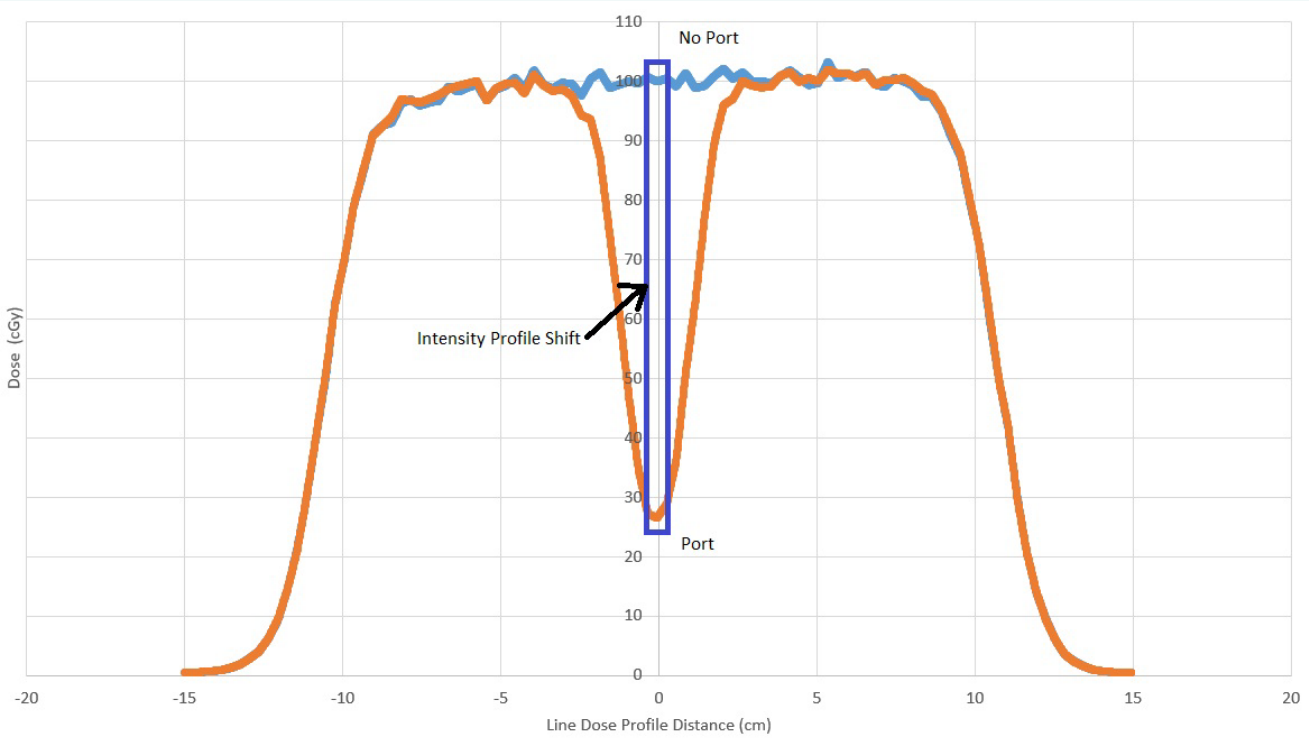

Figure 3 200 MeV proton beam intensity profile shift for an AngioDynamics® SmartPort+™ Plastic port.

Table 2. Dose intensity profile change for all ports at all energies.

	Dose Intensity Profile Change (%)							
	51 MeV		100 MeV		150 MeV		200 MeV	
Port	Difference	FWHM	Difference	FWHM	Difference	FWHM	Difference	FWHM
AngioDynamics® SmartPort+™ Plastic	-96%	1.74 cm	-70%	1.61 cm	-70%	2.03 cm	-75%	2.47 cm
BD® PowerPort® VUE M.R.I.®	-98%	2.26 cm	-91%	2.25 cm	-82%	2.32 cm	-82%	2.56 cm
BD® PowerPort ClearVUE® Slim®	-89%	1.79 cm	-82%	1.79 cm	-71%	1.92 cm	-67%	2.18 cm

The first metric in the data analysis was radiation measurements performed with an IBA Dosimetry® Model Zebra™ array. Radiation data was collected with and without a port in the beam to determine if the depth Bragg peak and related range shifted. Overall, the shift in this spectrum was similar for all ports. The change in the depth Bragg peak and related range was shallower, shifting left in the plot as an observed pull-back. Having ports in the therapeutic beam causes the depth Bragg peak to shift to a shallower depth, moving -0.6 cm to -1.4 cm. Results varied, depending on the port used and the energy of the proton beam. The position of the Bragg peak is critical to the understanding of how a SOBP can be created to treat a target cancer. It has been shown here that vascular access ports can change the position of the Bragg peak and the range of protons in the beam.

Range pull-back variations were observed during Zebra™ array single spot measurements. However, minimal variation was shown in large field treatment plan comparistion. This is because Zebra™ array measures integral depth dose (IDD), while central axis line doses were used in the plan comparison. For Mevion HyperScan system, spot size increases when energy decreases. Therefore, the ports impacts IDD differently with change of energy. Low energies are impacted more with their dose fall-off due to their spot size being larger than port itself.

Finally, data analysis was performed from a CT scan of the actual ports and modeled for dose in a RayStation® treatment planning system. For scenarios both with and without a port in the CT scan, modeling allowed for the determination of projected dose profiles perpendicular to the beam path. These profiles

permit understanding of how much dose change is exhibited in a normally flat beam. Changes in dose profile intensity were found to be high when ports were included in the beam. These intensity changes were simulated to be -67% to -95%. These findings are expected to have clinical relevance for physicians and medical physicists who are responsible for planning and dosing proton beam radiation therapy.

There are some limitations in this study. The measurement setting was different for 51 MeV as compared to other energies. The shallow depth setting of 51 MeV did not allow ports to be covered by additional bolus. For 100 MeV measurement, the thickness of the sandwiched setting was too thick for the range of the proton beam. The Zebra™ array measured dose out to about the depth of the 5% profile fall-off. Therefore, this increased difficulty of data fitting and range calculation. For non-uniform object like ports, the array can provide a rough estimation of range pull-back (more shallow-depth change on the plot), even though the treatment plan comparison is more accurate for such estimations.

Conclusions

Proton beam Bragg peaks and intensity profiles were analyzed for changes when a vascular access port was introduced into the path of the beam. Clinically available energies were considered from a cyclotron at 51 MeV, 100 MeV, 150 MeV and 200 MeV. Three different ports were investigated, including two commonly used ports from two different manufacturers. All three ports were known to be comprised primarily of, or entirely of plastics, which are understood to have lower density than ports constructed of primarily titanium. It was expected that this sample of ports would be appropriate to characterize the effect ports have on proton beams, since each were small in size and contained little, or no, high density metal components. Still, dosimetric analysis of proton beams with and without each port resulted in considerable dose changes. Dose variations were more pronounced at lower proton beam energies. Having ports in the therapeutic beam causes the depth Bragg peak to shift to a shallower depth, with the proton beam range moving as much as -0.6 cm to -1.4 cm. Finally, a high drop in profile intensity was observed at all proton beam energies, dropping the intensity from a normally flat profile down -67% to -96%. The FWHMs of the dose drop region varies between -1.70 cm and -2.60 cm.

No single port yielded results that suggest the ability to achieve optimal proton beam radiation therapy dosing when the beam traverses the port. Even though the ports evaluated were lower in density than ports constructed primarily of titanium, all three ports studied proved to alter the proton beam to levels that are expected to have clinical relevance. Clinical strategies for avoidance may include placement of dense implants at alternate sites away from the treatment area, removal of dense implants, or adjustment of the gantry angle to avoid the implant altogether, as recommended by the ACR.[15] Furthermore, knowledge of implant manufacturer, model, and design construction is useful in planning optimal care for patients in this setting. The current study may be considered by physicians and medical physicists who are responsible for chemoradiotherapy, PBT planning, dosing, and administration to optimize care delivery in this setting.

Acknowledgements

The corresponding author would like to thank the Proton.

Therapy Center at the Washington University School of Medicine for beam time, and AngioDynamics, Inc. for funding the study.

References

1. Broviac JW, Cole JJ, Scribner BH. “A silicone rubber atrial catheter for prolonged parenteral alimentation.” Surg Gynecol Obstet. 1973;136(4):602–06.
2. Dillon PA, Foglia RP. “Complications Associated with an Implantable Vascular Access Device.” Journal of Pediatric Surgery. 2006;41:1582-1587.
3. Johnson Kathleen A. Power Injectable Portal Systems. J Radiol Nurs. 2009;28:27-31.
4. Graham ML, Mutch LA, Rieke EF, Dunning Mm Zolondek EK, Faig AW, Hering BJ, Schuurman HJ. Refinement of Vascular Access Port Placement in Nonhuman Primates: Complication Rates and Outcomes. Comp Med. 2010;60(6):479-485.
5. Carroll PL. Reducing the risk of needlestick injury associated with implanted ports. Home Heathcare Nurse. 1998;16(4):225-234.
6. Rallis KS, Ho T, Yau L, Sideris M. Chemoradiotherapy in Cancer Treatment: Rationale and Clinical Applications. Anticancer Res. 2021;41(1):1-7.
7. Bagne FR, Merrick HW 3rd, Samsami N, and Dobelbower RR Jr. “Radiation dose perturbation in the presence of permanent vascular-access injection ports.” Int J Rad Oncol Biol Phys. 1990; 18(2):463–67.
8. Noriega BK, Feygelman V, Sanders RM. Radiation attenuation characteristics of venous access devices. Navan. 1994;1:12–14.
9. Gossman MS, Seuntjens JP, et al. “Dosimetric effects near implanted vascular access ports: an examination of external photon beam dose calculations.” J Appl Clin Med Phys. 2009;10(3):3-15.
10. Coll-Segarra D (2010). *Dosimetric effects near implanted vascular access ports under external electron beam radiation.* Wright State University Master’s Degree Thesis, Dayton, Ohio.
11. Gossman MS and Segarra DC. Electron radiation dosimetry for modern vascular access ports. Imaging Technology News. 2011;10:29-32.
12. Lehmkuhl L, Denecke T, Warschewske G, et al. “Multislice computed tomographic angiography for pre-interventional planning of port

placement for intra-arterial hepatic infusion chemotherapy." J Comput Assist Tomogr. 2007;31(1):66–71.

13. Gullane PJ. "Primary mandibular reconstruction: analysis of 64 cases and evaluation of interface radiation dosimetry on bridging plates." Laryngoscope. 1991; 101(6 Pt2 Suppl 54):1–24.

14. Hudson FR, Crawley MT, Samarasakera M. "Radiotherapy treatment planning for patients fitted with prostheses." Br J Radiol. 1984; 57(679):603–08.

15. ACR–ASTRO (2018). Practice Parameter for the Performance of Proton Beam Radiation Therapy. 1-20.

16. Charlie Ma, C-M; Lomax, Tony (2012). Proton and carbon ion therapy. Boca Raton: CRC Press. p. 4.

17. Chiang B-H, Bunker A, Jin H, Ahmad S, and Chen Y. (2020) Developing a Monte Carlo model for MEVION S250i with HYPERSCAN and Adaptive Aperture pencil beam scanning proton therapy system. Journal of Radiotherapy in Practice, p. 1.

18. Fisher S, Wuthrick E, Yu Y, Dicker AP. Horizons in Proton Therapy. Oncology Issues. 2009;Nov/Dec:23-25.

19. Zhao L, Cheng CW, Moskvin V, Wolanski M, James J, Gossman MS, Dikeman K, Srivastava S, and Das IJ. Dose uncertainty due to high-Z materials in clinical proton beam therapy. American Association of Physicists in Medicine, Philadelphia, PA, 2010;3295-3295, Poster abstract.

20. Basit Athar. Proton beam evaluation of common implantable port materials. Interventional Oncology Learning. Retrieved on May 11, 2023 from: https://www.hmpgloballearningnetwork.com/site/iolearning/white-papers/proton-beam-evaluation-common-implantable-port-materials. Published online 2021.